2024 IEEE International Conference on Robotics and Automation (ICRA 2024)
May 13-17, 2024. Yokohama, Japan

A Semi-Autonomous Data-Driven Shared Control Framework for Robotic Manipulation and Cutting of an Unknown Deformable Tissue

Nicholas A. Strohmeyer[1], Ji Hwan Park[2], Braden P. Murphy[2], and Farshid Alambeigi[2], *Member, IEEE*

***Abstract*— In this work, we propose a semi-autonomous scheme to synergistically share the complicated task of manipulation and cutting of an unknown deformable tissue (U-DT) between a remote surgeon and a surgical robot. Particularly, utilizing the da Vinci Research Kit (dVRK) platform, we have designed and successfully demonstrated a fully functional shared control scheme for an autonomous tensioning and tele-cutting of a U-DT. We have shown the system's ability to cooperate with a remote surgeon by leveraging an online data-driven learning and adaptive control method coupled with a reduced-order trajectory planning module that depends on just two parameters. By performing 25 experiments on custom-designed silicon phantoms and defining a set of success/failure metrics, we have put forward findings that establish a causal relationship between these two important parameters and the success or failure of the performed experiments.**

I. INTRODUCTION

The emergence of minimally invasive robotic surgery (MIRS), and particularly tele-surgical systems such as the da Vinci Robot, has greatly improved surgeons' comfort and precision. Meanwhile, as artificial intelligence (AI) becomes increasingly sophisticated, there are potential benefits to introducing autonomy into the surgical procedures performed on deformable tissues (DTs) [1]. While we are not yet at the point of performing fully autonomous surgeries on DTs– mainly due to the safety concerns– Autonomous Robot Surgical Assistants (ARSA) or semi-autonomous procedures can move us one step closer to this goal [2]. ARSA has the potential to partially automate certain surgical robotic procedures and *augment* a surgeon's ability during operation, thereby greatly reducing difficulty and improving the overall safety and outcomes of these procedures. [1], [2]. Furthermore, semi-autonomous systems have the advantage that they can utilize the experience, skills, and expertise of a surgeon while leveraging the precision and accuracy of robots. In this way, the robot and surgeon synergistically share responsibility of a complex surgical task.

Tissue debridement and surgical cutting could be a great candidate application for such synergistic collaborations. In current telesurgical cutting procedures, a surgeon uses one robot arm to grasp and manipulate the DT, creating tension, and facilitating the use of the other arm for cutting. Feedback is provided by the camera thus allowing the surgeon to *visually* analyze the deformation of the tissue and ensure the safety of the procedure . Nevertheless, due to the lack of reliable haptic feedback during manipulation, tissue tear and undesired incidents might occur during this tensioning and manipulation process [3].

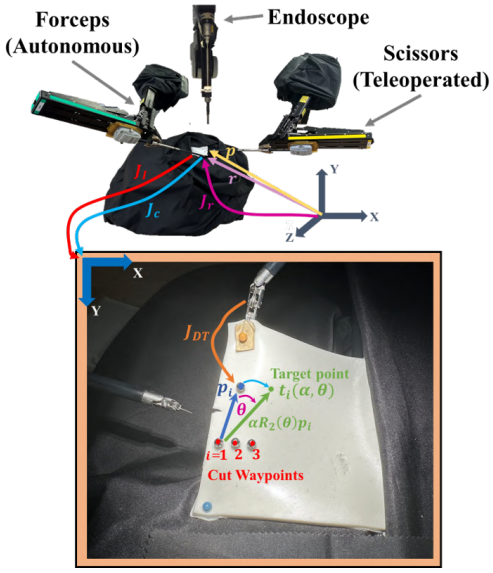

Fig. 1. Experimental setup shown to perform the semi-autonomous shared control manipulation and cutting tasks. As shown, the scissors are tele-manipulated by a remote surgeon and the forceps are autonomously controlled to manipulate a U-DT. In this setup, sewing pins mark feature points on U-DT and their respective projections into the image. The blue point marks the *reference point*, red points represent the *cut waypoints*, and the green point marks the current target point t_i. Parameters (α, θ) are used to define t_i, with respect to the current state and can be adapted over time to create general 2D trajectories. The system estimates J_{DT}, the Jacobian that maps the end effector to U-DT dynamics, and simultaneously uses this estimate to minimize the error between the reference and target points.

The current literature in this area documents a few efforts in which researchers have approached this problem through automating tissue manipulation (e.g., [4]–[7]) and cutting (e.g., [8]). Investigation of these efforts, however, reveals that most of these works have either been evaluated within simulated environments (e.g., [7]) or via experimental conditions that do not replicate a realistic surgical setting and real DT deformation behavior (e.g., [9]). More importantly, most of these works either have focused on the tissue manipulation or cutting tasks separately and have not formulated the entire task as a shared autonomy problem.

To address the above-mentioned limitations and as our main contributions in this work, we propose a novel, semi-autonomous scheme to synergistically share the complicated task of manipulation and cutting of an unknown deformable

[1]Department of Electrical and Computer Engineering, The University of Texas at Austin, Austin, TX, USA. E-mail: nstrohmeyer@utexas.edu

[2]Walker Department of Mechanical Engineering, Texas Robotics, The University of Texas at Austin, Austin, TX, USA. E-mail: {jihwanpark98, bradenpmurphy}@utexas.edu, Farshid.Alambeigi@austin.utexas.edu

tissue (U-DT) between a remote surgeon and a surgical robot. In the proposed bimanual procedure (pictured in Fig. 1), one arm is controlled autonomously to safely manipulate a U-DT and to provide proper tensioning while the surgeon tele-manipulates the other arm to perform the cutting. Notably, we leverage our previously published model-free framework [5], [6], [10], [11] in which a robot robustly learns the deformation behavior of a U-DT on-the-fly without having a-priori information of its mechanical properties.

A. Related Work

The shared autonomy modality is often studied from the angle of automating individual surgical subtasks. Examples include, but are not limited to, suturing [12] and shunt-insertion [13]. Studies like these have indicated the advantages of shared autonomy in reducing the mental workload of the surgeon during intensive MIRS procedures [14]. Thus far, to our knowledge, little or no work has been done to investigate a data-driven control framework within a shared autonomy context that addresses the manipulation and cutting steps concurrently. A more in depth review of the history of semi-autonomous systems in robotic surgery is given in [2].

Autonomous manipulation of DT is a hard problem due to the lack of a simple dynamics model which accurately represents the tissue and has been an active area of research. One popular approach is to train control policies within simulated environments using techniques from reinforcement learning [9]. While the modeling of DT in a simulated environment is a common practice due to its convenience and the evidence of the efficacy of simulations as a practical training tool. Also, these methods can suffer from the sim2Real problem and it is unclear how well they can generalize to unseen, real-world scenarios. Other works have explored alternative training regimes such as learning by demonstrations. For instance, in [15], the method was combined with model-predictive control to effectively carry out Point-Based Indirect Positioning (PBIP) [6], [16]. Such methods, however, are still somewhat indirect as the autonomous agent learns a representation of the U-DT through the intermediary of human actions in a similar context. Model-free methods offer another type of approach altogether. These methods which aim to learn the dynamics of tissue directly through interaction, often integrating visual information picked up by camera as well. Some notable examples of model-free tissue manipulation are based on real-time available data in order to simultaneously learn and deploy a Jacobian matrix, which has been proven effective in PBIP [10], [11].

II. PROBLEM STATEMENT AND ASSUMPTIONS

Let us assume a surgeon is using a tele-surgical robotic system, such as the da Vinci Surgical system, to perform a robotic tissue manipulation and cutting task. As illustrated in Fig. 1, the primary objective is to develop a shared control framework for semi-autonomous manipulation and cutting of a U-DT. In our formulation, the *primary*, more sensitive task of cutting is given to the surgeon through a teleoperated

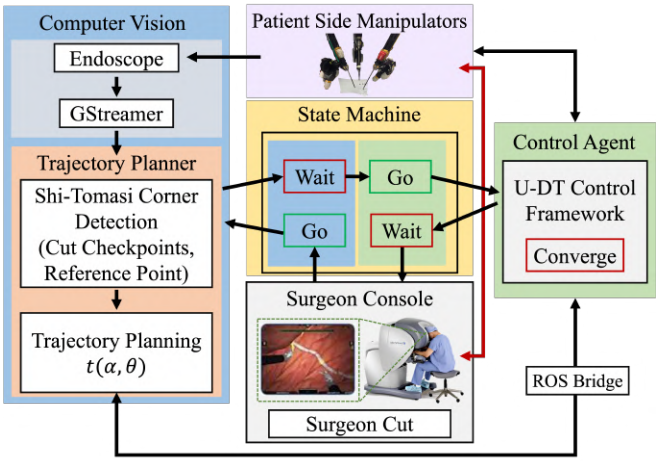

Fig. 2. The architecture of the proposed shared autonomy framework for surgical cutting. In each envisioned cycle, the trajectory planner begins the process by planning a point in the image plane while the control module waits. Upon receiving the target point, control module activates and performs PBIP to align the reference with the target. When points are converged, the ARSA goes back into the "waiting" state while the surgeon advances the cut along to the next waypoint.

mode and the *auxiliary* manipulation and tensioning task is given to the autonomous robotic agent. Thus, the ARSA must manipulate a U-DT without endangering patient's safety while helping the surgeon to accomplish the cutting task.

To accomplish this objective, we make the following assumptions: (i) We assume throughout the process, we have access to a steady RGB video feedback provided by the endoscope, shown in Fig. 1; (ii) We assume the feature points, including the reference point and the cut waypoints, shown in Fig. 1, are predefined and visible to tracking algorithms at all stages of the procedure. Also, the cuts performed by the remote surgeon are assumed to be optimal under the given circumstances. It is worth emphasizing that we do *not* assume any known properties for the deformable tissue *a priori*. The dynamics mapping from end effector displacements to U-DT displacements is also unknown and must be estimated on the fly. Furthermore, in our proposed approach the camera does not need to be calibrated *a priori* as its calibration parameters are also estimated within the proposed method. Two key challenges our design must address are **(i)** allowing the remote surgeon to work synchronously with the ARSA; and **(ii)** providing a robust control policy to the ARSA for safe and effective completion of the auxiliary tensioning task. Our solution to these challenges is addressed in the following section and is visually summarized by Fig. 2.

A. Shared Control Flow

A shared autonomy design requires proper coordination of the flow of the procedure. In our design, this task is accomplished by a simple state machine which tracks this flow, facilitates communication between modules, and ensures the modules perform their functions at the proper times. Furthermore, an operator oversees the overall safety and flow of the procedure from the computer and activates the autonomous agent at every step. The process begins

when the camera is first activated and feature points received. Based on this input, the trajectory planner decides the goal state (shown by a green point in Fig. 1) given the current positions of said feature points. Next, the operator activates the ARSA's control module which smoothly manipulate the U-DT to the desired goal state. The surgeon acts next and indicates to the operator, when ready, for the agent to activate again. The next goal state is planned, and the process is repeated.

B. Computer Vision Module

The computer vision (CV) module is responsible for tracking the U-DT feature points (shown in Fig. 1), which represent the state of the task. The U-DT feature points include a single reference point placed near the robot gripper (i.e., blue point in Fig. 1) and a set of cut waypoints (i.e., red points in Fig. 1), which are used to describe a given desired cut trajectory. Crucially, the reference point is passed to the control algorithm which works by aligning it with target point in image space at each step. As shown in Fig. 2, the CV module is comprised of several components including the Shi-Thomasi algorithm, which obtains the image coordinates of the feature points at the start of each step of the procedure, and the Lucas-Kanade optical flow algorithm, which is then used to track these coordinates during the manipulation phase [6]. The feature points are physically marked on the U-DT by sewing pins, which are colored with a special crossing pattern to enable the functionality of our selected cv algorithms.

C. Trajectory Planning Module

Trajectory planning is a key design feature as it indirectly encodes the manipulation behavior and safety of the procedure by providing the ARSA a reference path to follow through image space. In prior works, [5], [10], [11], a static goal point is predefined by the surgeon. This would be limiting for application to a synergistic tissue manipulation and cutting task. Therefore, we extend this framework to an *iterative*, reduced-order planning approach. Rather than using a predefined, constant target point (i.e., green point in Fig. 1), its location is updated using the current position of desired cut waypoints (i.e., red points in Fig. 1), the reference point (i.e., blue point in Fig. 1), and the current step of the procedure. Specifically, the target locations $t_i \in \mathbb{R}^2$ are calculated as follows:

$$t_i(\theta, \alpha) = \alpha . R_\theta . \mathbf{p_i} \tag{1}$$

where $\mathbf{p_i} \in \mathbb{R}^2$ is the vector from the current waypoint to the reference point in the image plane. $R_\theta \in \mathbb{R}^{2\times 2}$ rotates $\mathbf{p_i}$ through an angle of θ about the z axis while $\alpha \in \mathbb{R} > 0$ scales its magnitude. The tuple (α, θ) encodes these operations on $\mathbf{p_i}$ and thus defines the next goal point g_i w.r.t. to the current state.

While performing the auxiliary task of tensioning, the ARSA must always pull the U-DT in a "safe" direction. Since the tension created is implicit in the definition of the trajectory that it follows, we have the notion that input parameters are directly related to a "safe" region of manipulation. Similarly, a notion of parameter optimality could be defined. We return to these points in the Experiment section.

D. Control Module

As depicted in Fig. 2, the model-free autonomous learning and manipulation of the U-DT runs inside an inner loop of the proposed architecture. The control module operates upon the single goal point g_i and a consistent stream of reference point coordinate updates from the CV module. U-DT manipulation is achieved using the data-driven learning framework from [5], [11]. The function maps small 3-dimensional displacements in the task space to small 2-dimensional displacements in image space can be modeled as an unknown Jacobian matrix $\mathbf{J}_I \in \mathbb{R}^{2\times 3}$. Likewise, $\mathbf{J}_{DT} \in \mathbb{R}^{3\times 3}$, models the function mapping between end effector actuation $\Delta\mathbf{r} \in \mathbb{R}^3$ and small displacements of the reference point $i(t)$ on the U-DT. Thus, the matrix product $\mathbf{J}_I\mathbf{J}_{DT}$ defines a *combined* Jacobian matrix $\mathbf{J}_c \in \mathbb{R}^{2\times 3}$ which is an approximate map from robot actuation to the displacement of the reference point ($\Delta\mathbf{i}$) in image space:

$$\Delta\mathbf{i}(t) \approx \mathbf{J}_c(t)\Delta\mathbf{r}(t)$$

where $\Delta\mathbf{i}(t) = [\Delta\mathbf{x}(t); \Delta\mathbf{y}(t)] \in \mathbb{R}^2$. Rather than calculate J_c directly, it is estimated online, at every iteration, using Broyden's update rule [5]:

$$\widehat{\mathbf{J}_c}(t+\Delta t) = \widehat{\mathbf{J}_c}(t) + \psi \frac{\Delta\mathbf{i}(t) - \widehat{\mathbf{J}_c}(t)\Delta\mathbf{r}(t)}{\Delta\mathbf{r}(t)^\intercal \Delta\mathbf{r}(t)} \Delta\mathbf{r}(t)^\intercal \tag{2}$$

where $0 \leq \psi \leq 1$ is a constant parameter, controlling the rate of change of $\widehat{\mathbf{J}_c}$ [5].

The estimate $\widehat{\mathbf{J}_c}$ is used to minimize the distance between the reference point $i(t)$ and goal point g_i (i.e., $\Delta\eta(t) = g_i - i(t)$) while simultaneously minimizing change in the robot's joint space $\Delta\mathbf{q}$. This is formulated as the following adaptive optimization problem:

$$\underset{\Delta\mathbf{q}(t)}{\arg\min} \quad \left\| \widehat{\mathbf{J}_c}(\mathbf{r}(t))\Delta\mathbf{r}(t) - \Delta\eta(t) \right\|_2^2 + \omega \left\| \Delta\mathbf{q}(t) \right\|_2^2 \tag{3}$$

E. Evaluation and Success Metrics

1) Characterizing Success: We characterize successes and failures of the proposed shared control framework under various input parameters across identical conditions. In the performed sequential cutting procedures and at each step of process, a *success* is defined as a case in which the surgeon completes a cut through the tele-operation mode and we are able to proceed to the next step. We follow a specific criteria for marking each step either a success or failure according to four possible modes which are defined in the Results section.)

2) Manipulation Metrics: The *first* metric is the *Point Position Error* (henceforth referred to as PPE), which is the Euclidean distance between the reference p_i and target points t_i in the image plane (see Fig. 1). *Second* metric is *Yoshikawa's Manipulability Metric* (Ω and henceforth

abbreviated as YMM) of the combined Jacobian matrix J_c. The calculation is given below.

$$\text{YMM} = \sqrt{det(\widehat{J_C}\ \widehat{J_C^{\intercal}})} \tag{4}$$

In the *Third* metric, we calculate ΔYMM which is the difference in YMM at successive iterations ($\text{YMM}_{k+1} - \text{YMM}_k$).

III. EXPERIMENT DESIGN

A. Physical Setup

we have several notable features, which support the feasibility of our methods for real-world settings. First, we fabricated dozens of $101mm \times 101mm$ rectangular silicone phantoms to serve as the U-DT in our experiment. The silicone mixture made of 1:1 ratio of two part Smooth-On Ecoflex 00-35 Fast Platinum Cure Silicone (Smooth-On Inc.). Each phantom's thickness varied between 1.4 and 1.6 mm and its mass between 20 and 22 g. Second, we tested our semi-autonomous framework using the da Vinci Research Kit (dVRK) [17], developed by the researchers at Johns Hopkins University, along with its open-source software[1] (cisst/SAW) and electronics. The experiment required two patient side manipulators (PSMs), where the left PSM was equipped with EndoWrist® ProGrasp™ Forceps (Intuitive Surgical, Inc., California, USA) and the right PSM was equipped with EndoWrist® round tip scissors. The forceps grasp and manipulate the U-DT while the scissors are teleoperated by a human surgeon who directs the cutting task using a Master Tool Manipulator (MTM). A single Endoscopic Camera Manipulator (ECM) equipped with a stereo camera was also used to provide visual feedback and fed the control framework and surgeon console. The full configuration is visualized in Fig. 1 For each run of the experiment, we set the length of the target cut trajectory to 40 mm from the edge of a phantom. Three cut pins were evenly spaced to span this distance. The reference pin was placed an additional 40 mm relative to the line of cut waypoints near the grasp point. The endoscope was held at a constant distance of 150 mm above the task space so as to ensure a near-identical view across trials.

B. Classification of Modes

We identified and defined 4 key modes, which characterized a successful trial. For a visual understanding, the reader can refer to Fig. 3.

Mode 1: Tearing (T) means the U-DT is over-actuated during the online learning and manipulation control algorithm described in Section II-D, causing either an actual tear or an unnecessary level of stretching in the U-DT near the cut site. This case is not only classified as a failure but also poses the greatest risk of harm to the patient.

Mode 2: Folding (F) is the opposite extreme, in which the tissue is critically under-actuated. The ARSA has either folded the tissue over the target point in an effort to converge to the desired target point defined by (1), obscuring the cut site, or there is significant bending in the tissue near the cut site, making future cuts exceedingly difficult or not possible without a reset.

Mode 3: System Failure (Sys) is recorded if the CV module loses track of feature points, the reference point leaves the image frame, the PSM is obstructed in task space, or any other such edge case requires a stoppage occurs.

Mode 4: Success (S) is defined as absence of any of the preceding failure modes. In a successful trial, the proposed framework exhibits generally "good" behavior, such that the surgeon is able to complete the cut at all 3 stages safely and without need for resetting.

[1]https://github.com/jhu-dvrk/sawIntuitiveResearchKit

TABLE I
EXPERIMENTS SUMMARY

α *	θ *	Success	Tear	Fold	System	Total
1.1	5	1	0	0	1	2
	10	2	0	2	1	5
	20	0	0	1	0	1
	30	0	0	2	0	2
1.2	5	1	1	0	0	2
	10	3	1	0	1	5
1.3	5	0	2	0	2	2
	10	1	0	0	0	1
	20	0	0	1	1	2
1.4	5	0	1	0	0	1
	10	0	1	0	0	1
1.5	5	0	1	0	0	1

* α is a dimensionless scale factor, θ is in degrees

C. Parameter Trials

To study the efficacy of the proposed framework and particularly the planning module on the performance of the semi-autonomous shared control framework, we conducted a total of $k = 25$ experiments with different (α_k, θ_k) tuples. As described, in this study, we were particularly interested in identifying the optimal combination of (α_k, θ_k)– defining the appropriate target points t_i in the image plane– that provides sufficient tension for the remote surgeon to sequentially perform the cutting procedure. To define which combinations (α_k, θ_k) to use for the experiment, we begin with an empirical search. Initial bounds on parameters were chosen during an offline planning phase in which we scanned a range of parameters and plotted their corresponding waypoint trajectories overlaying the endoscope image. From this, we identified a bounded region of the parameter space for testing. We sampled $(alpha_k, theta_k)$ pairs at regular intervals across this region and conducted live shared autonomy trials. The outcomes of these trials are summarized in Table I. Videos of the conducted experiments were recorded for further analysis and can be viewed in the accompanied multimedia with this manuscript.

IV. DISCUSSION OF RESULTS

Our results demonstrate the feasibility of the shared autonomy framework. Given proper tuning of input parameters (α, θ) to the low-dimensional planning module, the ARSA and human surgeon are able to cooperate successfully to safely complete the task. Fig. 4 provides a particularly intuitive visualization of the connection between these parameters and experimental outcomes. Note that C_{Mode}^{Step} labels

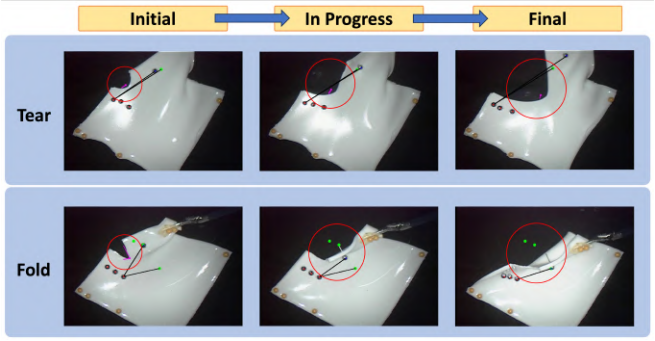

Fig. 3. The progression of both *tearing* and *folding* failure modes throughout two sample failure experiments.

the outcome mode at each corresponding step of the trial. For example, C_T^2 refers to a tear at step 2 of the experiment. There are three distinct stpes corresponding to three defined cut waypoints. Furthermore, using the numerical data from Table I, we provide estimated regions of low and high probability of success in parameter space (i.e., possible tuple (α, θ) combinations) in Fig. 4. To calculate this estimate, we used the following procedure: for each sampled parameter pair $p = (\alpha, \theta)$ at step $j \in 1, 2, 3$, we recorded a binary result $X_j^p \in \{0, 1\}$ (success/failure) and took the sample mean for each (p, j). To balance for sensitivity to small sample sizes, we took the sum of the sample mean for each (p, j) and the proportion of total success cases (S_j) at step j accounted for by that particular pair p. The final estimate was given by the following:

$$Q_p^j = \frac{\Sigma_i X_i^p}{N_j^p} + \frac{\Sigma X_i^p}{S_j} \tag{5}$$

where N_j^p is number of trials for test parameters p at step j. Normalizing Q_p^j and linearly interpolating over missing regions of parameter space generates the heat maps shown in Fig. 4

A. Metrics Analysis

We now move to an analysis of the three aforementioned metrics: PPE, YMM, and ΔYMM which convey the system's level of difficulty in reducing error, the state of the U-DT under actuation, and the instantaneous changes in state, respectively. These metrics are also given in Fig. 4 for exemplary failure and success modes. Their corresponding input parameters are marked by color-coded $\star$'s on the heat map.

1) Analyzing a Typical Success: Success was often accompanied by smooth changes in the reference YMM and a relatively flat or decreasing value across iterations of a single tensioning phase. Small upticks may exist while the algorithm explores, but these are brief and smoother than comparable failure modes (i.e., C_S^1 v. C_T^1 in Fig. 4). Smoothness is more clearly demonstrated by the ΔYMM plots in Fig. 4. Notably, PPE is consistently and linearly decreasing to 0.

2) Analyzing Typical Failures: Large positive spikes in ΔYMM are most associated with tearing or "over-pulling", as well as sustained increases in YMM, as seen in C_T^1 and C_T^2 trials in Fig. 4. This result lends some intuition. Increasing YMM indicates greater manipulability, which, in our setting, correlates with increasing stiffness. Assuming the initial state at each step is not far from optimal, steadily increasing values would serve as a warning that the system is moving farther and farther away from safety until a tear ultimately occurs. At the other extreme, we see that folding also tends to produce turbulent sequences in the YMM series when compared with the ideal case, although sharp changes are less pronounced than in the case of tearing. While changes happen suddenly in tearing cases, we saw more oscillatory behavior with folding as in C_F^1. Practically, this meant the system was searching for actions to proceed toward its goal of minimizing error but was often met with difficulty due to physical limits. This is also reflected in the PPE, which "flattens", taking much longer to converge (if at all), as seen in C_F^2 trial, especially. In fact, PPE seems to be a powerful predictive signal of failure for both modes. In cases C_F^2 C_F^3 and C_T^3, there is clear flattening or "drifting" of PPE. This indicates an implicit issue with the definition of the goal point causing the system to struggle to converge. The error stops decreasing up until a sudden (usually undesirable) change occurs. Thus, a flattening error curve was observed to be a reliable signal of undesirable behavior across all failure modes.

V. CONCLUSION

In this paper, we have designed and successfully demonstrated a fully functional shared control scheme for an autonomous tensioning and tele-cutting of a U-DT using the dVRK platform. We have shown the system's ability to cooperate with a remote surgeon using an online adaptive control combined with a reduced-order trajectory planning module that depends solely on two tunable parameters (α, θ). Through our 25 experiments and definition of relevant metrics, we have put forward findings that establish a causal relationship between these two important parameters and the success or failure of the performed experiments.

Despite the features of the proposed shared-control framework, the size of the data set collected for this paper is a key limitation. While we believe we have identified important trends, more experiments would increase confidence. A more complete analysis of our system might include a greater variety of fabricated U-DT's. Furthermore, our collection of feedback signals need not be limited to a single point on the U-DT. In future work, we plan to make these enhancements and, furthermore, design methods using this richer dataset for online adaptation of the parameters (α, θ) for real-time optimization, which may be preferable to the method of empirical search and sampling used in our experiments here. We also are interested in sampling YMM at a larger set of points than the single reference point in order to construct fuller information about tissue dynamics.

REFERENCES

[1] M. Yip and N. Das, "Robot autonomy for surgery," in *The Encyclopedia of MEDICAL ROBOTICS: Volume 1 Minimally Invasive Surgical Robotics*, pp. 281–313, World Scientific, 2019.

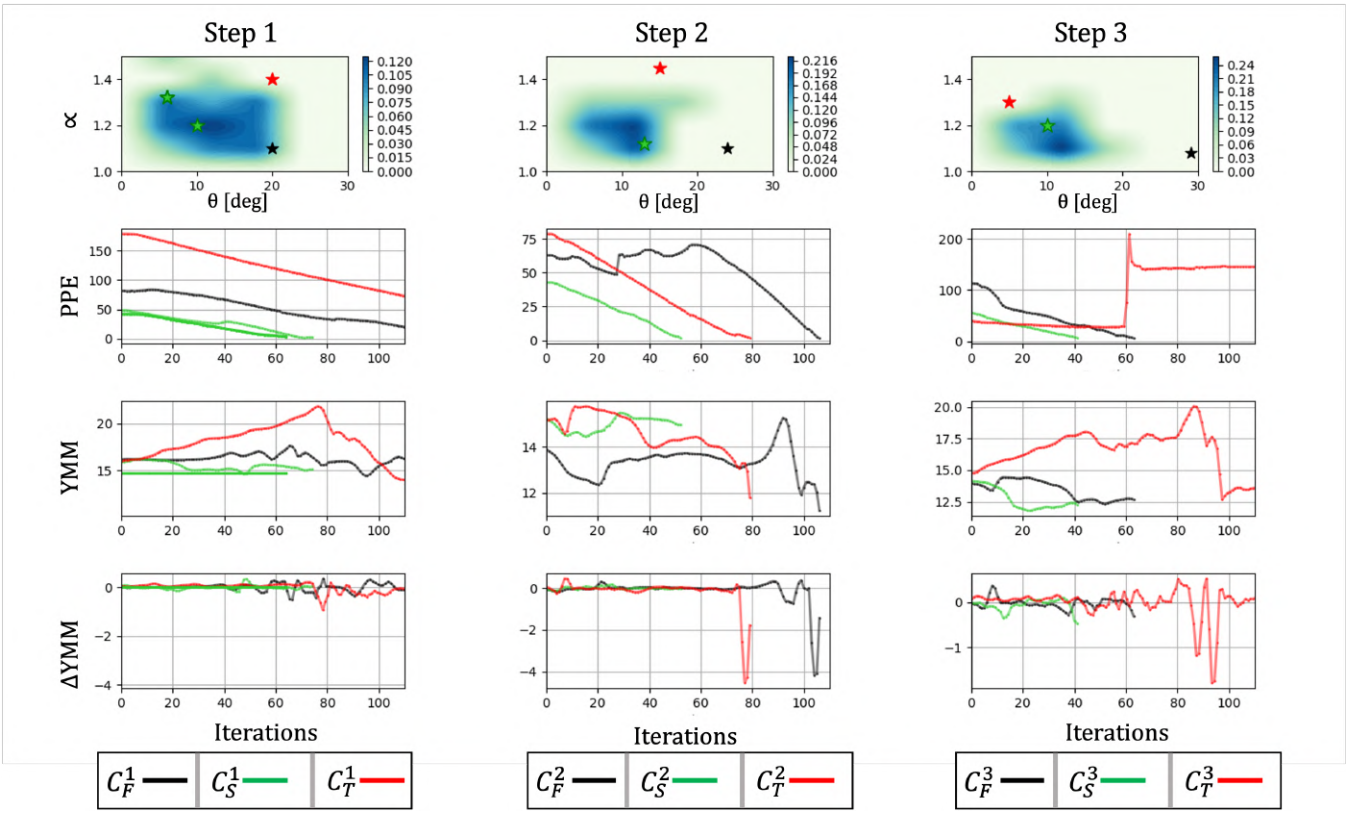

Fig. 4. The first row depicts an estimated likelihood of success for a given (α, θ) combination at a given step in the procedure. Darker regions indicate a higher probability of success. The next three rows are PPE, YMM, ΔYMM and overlay three relevant modes in our discussion: success, tear and fold. Each time series in rows 2-4 are color-coded and corresponded to points plotted in row 1. In stage 1, we selected 2 success examples to demonstrate a wider feasible region. This feasible region narrows and shrinks down as cutting progresses and the U-DT becomes less elastic.

[2] T. Haidegger, "Autonomy for surgical robots: Concepts and paradigms," *IEEE Transactions on Medical Robotics and Bionics*, vol. 1, no. 2, pp. 65–76, 2019.

[3] J. Zhu, A. Cherubini, C. Dune, D. Navarro-Alarcon, F. Alambeigi, D. Berenson, F. Ficuciello, K. Harada, X. Li, J. Pan, *et al.*, "Challenges and outlook in robotic manipulation of deformable objects," *arXiv preprint arXiv:2105.01767*, 2021.

[4] A. Shademan, R. S. Decker, J. D. Opfermann, S. Leonard, A. Krieger, and P. C. Kim, "Supervised autonomous robotic soft tissue surgery," *Science translational medicine*, vol. 8, no. 337, pp. 337ra64–337ra64, 2016.

[5] F. Alambeigi, Z. Wang, Y.-h. Liu, R. H. Taylor, and M. Armand, "Toward semi-autonomous cryoablation of kidney tumors via model-independent deformable tissue manipulation technique," *Annals of Biomedical Engineering*, pp. 1–13, 2018.

[6] F. Alambeigi, Z. Wang, R. Hegeman, Y.-H. Liu, and M. Armand, "Autonomous data-driven manipulation of unknown anisotropic deformable tissues using unmodelled continuum manipulators," *IEEE Robotics and Automation Letters*, vol. 4, no. 2, pp. 254–261, 2018.

[7] S. A. Pedram, P. W. Ferguson, C. Shin, A. Mehta, E. P. Dutson, F. Alambeigi, and J. Rosen, "Toward synergic learning for autonomous manipulation of deformable tissues via surgical robots: An approximate q-learning approach," in *2020 8th IEEE RAS/EMBS International Conference for Biomedical Robotics and Biomechatronics (BioRob)*, pp. 878–884, IEEE, 2020.

[8] T. Nguyen, N. D. Nguyen, F. Bello, and S. Nahavandi, "A new tensioning method using deep reinforcement learning for surgical pattern cutting," in *2019 IEEE international conference on industrial technology (ICIT)*, pp. 1339–1344, IEEE, 2019.

[9] B. Thananjeyan, A. Garg, S. Krishnan, C. Chen, L. Miller, and K. Goldberg, "Multilateral surgical pattern cutting in 2d orthotropic gauze with deep reinforcement learning policies for tensioning," in *2017 IEEE International Conference on Robotics and Automation (ICRA)*, pp. 2371–2378, IEEE, 2017.

[10] M. Retana, K. Nalamwar, D. T. Conyers, S. F. Atashzar, and F. Alambeigi, "Autonomous data-driven manipulation of an unknown deformable tissue within constrained environments: A pilot study," in *2022 International Symposium on Medical Robotics (ISMR)*, pp. 1–7, IEEE, 2022.

[11] B. P. Murphy and F. Alambeigi, "A surgical robotic framework for safe and autonomous data-driven learning and manipulation of an unknown deformable tissue with an integrated critical space," *Journal of Medical Robotics Research*, p. 2340001, 2023.

[12] S. Sen, A. Garg, D. V. Gealy, S. McKinley, Y. Jen, and K. Goldberg, "Automating multi-throw multilateral surgical suturing with a mechanical needle guide and sequential convex optimization," in *2016 IEEE international conference on robotics and automation (ICRA)*, pp. 4178–4185, IEEE, 2016.

[13] K. Dharmarajan, W. Panitch, B. Shi, H. Huang, L. Y. Chen, T. Low, D. Fer, and K. Goldberg, "A trimodal framework for robot-assisted vascular shunt insertion when a supervising surgeon is local, remote, or unavailable," in *2023 International Symposium on Medical Robotics (ISMR)*, pp. 1–8, IEEE, 2023.

[14] S. Kumar, D. H. Liu, F. S. Racz, M. Retana, S. Sharma, F. Iwane, B. P. Murphy, R. O'Keeffe, S. F. Atashzar, F. Alambeigi, *et al.*, "Cognidavinci: Towards estimating mental workload modulated by visual delays during telerobotic surgery-an eeg-based analysis," in *2023 IEEE International Conference on Robotics and Automation (ICRA)*, pp. 6789–6794, IEEE, 2023.

[15] C. Shin, P. W. Ferguson, S. A. Pedram, J. Ma, E. P. Dutson, and J. Rosen, "Autonomous tissue manipulation via surgical robot using learning based model predictive control," in *2019 International conference on robotics and automation (ICRA)*, pp. 3875–3881, IEEE, 2019.

[16] F. Alambeigi, Z. Wang, R. Hegeman, Y.-H. Liu, and M. Armand, "A robust data-driven approach for online learning and manipulation of unmodeled 3-d heterogeneous compliant objects," *IEEE Robotics and Automation Letters*, vol. 3, no. 4, pp. 4140–4147, 2018.

[17] P. Kazanzides, Z. Chen, A. Deguet, G. S. Fischer, R. H. Taylor, and S. P. DiMaio, "An open-source research kit for the da vinci® surgical system," in *2014 IEEE international conference on robotics and automation (ICRA)*, pp. 6434–6439, IEEE, 2014.